Space-Charge Limited Photocurrent

V. D. Mihailetchi, J. Wildeman, and P. W. M. Blom

Molecular Electronics, Materials Science Centre, University of Groningen, Nijenborgh 4, NL-9747 AG Groningen, The Netherlands

(Received 8 December 2004; published 1 April 2005)

In 1971 Goodman and Rose predicted the occurrence of a fundamental electrostatic limit for the photocurrent in semiconductors at high light intensities. Blends of conjugated polymers and fullerenes are an ideal model system to observe this space-charge limit experimentally, since they combine an unbalanced charge transport, long lifetimes, high charge carrier generation efficiencies, and low mobility of the slowest charge carrier. The experimental photocurrents reveal all the characteristics of a space-charge limited photocurrent: a one-half power dependence on voltage, a three-quarter power dependence on light intensity, and a one-half power scaling of the voltage at which the photocurrent switches into full saturation with light intensity.

DOI: 10.1103/PhysRevLett.94.126602 PACS numbers: 72.80.Le, 73.61.Ph

When a semiconductor is exposed to photons with an energy larger than the band gap, charge carriers are produced. With a built-in field or an externally applied bias these charge carriers can be separated, thereby producing a photocurrent in an external circuit. The efficiency of photocurrent generation depends on the balance between charge carrier generation, recombination, and transport. The extraction of photogenerated electrons and holes from a semiconductor has been treated by Goodman and Rose [1]. With noninjecting contacts the external photocurrent becomes saturated when all photogenerated free electrons and holes are extracted from the semiconductor. This implies that the mean electron and hole drift lengths $w_{e(h)} = \mu_{e(h)}\tau_{e(h)}E$ are equal to or longer than the specimen thickness L: with $\mu_{e(h)}$ the charge carrier mobility of electrons (holes), $\tau_{e(h)}$ the charge carrier lifetime, and E the electric field, respectively. In this case no recombination occurs and the saturated photocurrent density (J_{ph}) is given by $J_{\mathrm{ph}}^{\mathrm{sat}} = qGL$, with G the generation rate of the electron-hole pairs and q the electric charge [1]. However, if $w_e < L$ or $w_h < L$ or both are smaller than L, space charge will form and the recombination of free charge carriers becomes significant.

Suppose now that the electron-hole (e-h) pairs are photogenerated uniformly throughout the specimen and that the charge transport is strongly unbalanced, meaning that $w_e \neq w_h$. In a semiconductor with $w_h \ll w_e$ and $w_h < L$, the holes will accumulate to a greater extent in the device than the electrons, which makes the applied field nonuniform. As a consequence, the electric field increases in the region (L_1) near the anode, enhancing the extraction of holes, as shown schematically in the inset of Fig. 1. Conversely, in the region near the cathode the electric field decreases, diminishing the extraction of electrons. In steady state, the electric field in the region with thickness L_1 is modified to such an extent that the external hole current equals the external electron current. The length of the region L_1 is given by the mean hole drift length ($L_1 = \mu_h\tau_h V_1/L_1$). Since almost the entire voltage V drops on the region of hole accumulation ($V_1 \approx V$) and the photocurrent generated in this region is substantially the total current, it follows directly that [1]

$$J_{\mathrm{ph}} = qGL_1 = qG(\mu_h\tau_h)^{1/2}V^{1/2}. \quad (1)$$

It is evident that in the region L_1 the accumulated holes are not neutralized by an equal density of electrons, which results in a buildup of positive space charge. Goodman and Rose pointed out that there is a fundamental limit to be expected for the buildup of space charge in a semiconductor at high intensities. The electrostatic limit of hole accumulation is reached when the photocurrent generated in this region, $J_{\mathrm{ph}} = qGL_1$, is equal to the space-charge limited current:

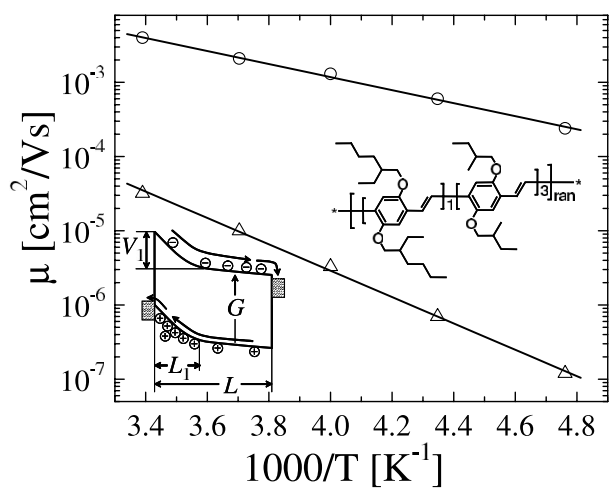

FIG. 1. Experimental charge carrier mobility of the electrons (μ_e, ○) and holes (μ_h, △) as a function of temperature T. The μ_e and μ_h have been determined from space-charge limited measurements on 20:80 blends of BEH_1BMB_3-PPV:PCBM. The inset schematically shows a photovoltaic device under illumination and the chemical structure of the BEH_1BMB_3-PPV, respectively.

 © 2005 The American Physical Society

$$J_{\mathrm{SCL}} = \frac{9}{8}\varepsilon_0\varepsilon_r\mu_h\frac{V_1^2}{L_1^3}, \tag{2}$$

where $\varepsilon_0\varepsilon_r$ is the dielectric permittivity. By equating qGL_1 with Eq. (2) it follows that the length of the region L_1 in this space-charge limited (SCL) regime is given by

$$L_1 = (9\varepsilon_0\varepsilon_r\mu_h/8qG)^{1/4}V_1^{1/2}. \tag{3}$$

Since $V_1 \approx V$, the maximum electrostatically allowed photocurrent that can be extracted from the device is [1]

$$J_{\mathrm{ph}} = q\left(\frac{9\varepsilon_0\varepsilon_r\mu_h}{8q}\right)^{1/4}G^{3/4}V^{1/2}. \tag{4}$$

Comparison of Eqs. (1) and (4) shows that in both the absence and the presence of the space-charge limitation J_{ph} scales with the square root of the applied voltage and is governed by the slowest charge carrier mobility, although the physical reasons for this are distinctly different. Experimentally, both regimes can be discriminated by investigating their dependence on G.

To our knowledge, the existence of SCL photocurrents has not been demonstrated experimentally in semiconductors so far. In order to observe SCL photocurrents, a semiconductor should fulfill a number of requirements: First, the amount of photogenerated charge carriers should be large, meaning a large G and a long carrier lifetime $\tau_{e(h)}$ after dissociation of the e-h pairs. Furthermore, the charge transport should be strongly unbalanced, leading to the formation of space-charge regions. Finally, the slowest charge carrier should have a low mobility such that the photocurrent can reach the SCL current inside the space-charge region. A material system that fulfills most of these demands are blends of conjugated polymers (electron donor) and fullerene molecules (electron acceptor) [2], which exhibit power-conversion efficiencies of 3% under global AM1.5 illumination [3]. In these blends light absorption leads to the production of excitons that subsequently dissociate at the internal interface by an ultrafast electron transfer (< 100 fs) from excited polymer to fullerene [4]. Since the created electrons and holes are spatially separated, the backtransfer process is very slow, leading to long-lived charge carriers, in the microsecond to millisecond range [5,6]. In combination with the large internal donor-acceptor interface, these bulk heterojunctions enable a large generation rate of long-lived charge carriers.

In this study, we have investigated the photocurrent of blends using a poly(p-phenylene vinylene) (PPV) derivative and [6,6]-phenyl C_{61}-butyric acid methyl ester (PCBM). We demonstrate that the photocurrent in this conjugated polymer and fullerene blend reaches the fundamental space-charge limit when the difference in electron and hole mobilities exceeds 2 orders of magnitude, even under normal light intensity (at 0.8 Sun illumination). The occurrence of this upper limit for the photoconduction under normal light intensity is of importance for the understanding and further optimization of photovoltaic devices based on these material systems.

The important quantity that determines the formation of space charge in photoconductors is the difference in the $\mu\tau$ products of electrons and holes. The most investigated system of polymer-fullerene solar cells are blends of poly[2-methoxy-5-(3′,7′-dimethyloctyloxy)-p-phenylene vinylene] (OC_1C_{10}-PPV) and PCBM. The main recombination process found in these devices is bimolecular recombination of photogenerated free electrons and holes [7], resulting in an equal electron and hole lifetime. Therefore, a large mobility difference between electrons and holes is required for the generation of a SCL photocurrent in this system. However, it turns out that the hole mobility of OC_1C_{10}-PPV inside the blend is enhanced by a factor of 400 as compared with the pure material [8]. The resulting mobility difference of only 1 order of magnitude is not sufficient to induce a SCL photocurrent. In the present study the random copolymer poly[2,5-bis(2′-ethylhexyloxy)-co-2,5-bis(2′-methylbutyloxy)-1,4-phenylene vinylene] (BEH_1BMB_3-PPV) is used, with its chemical structure shown in the inset of Fig. 1. For this symmetrically substituted PPV, when blended with PCBM, we observe that the hole mobility in the PPV phase is hardly affected, resulting in an increased mobility difference between electrons and holes. The measurements were performed on 20:80 weight percentage blends of BEH_1BMB_3-PPV:PCBM sandwiched between two electrodes with an asymmetric work function, which are noninjecting under reverse bias operation. A reverse voltage sweep from 1 V down to -12 V has been applied and the current density under illumination (J_L) and in the dark (J_D) has been recorded. The experimental photocurrent is given by $J_{\mathrm{ph}} = J_L - J_D$. From the resulting $J_{\mathrm{ph}} - V$ characteristics the compensation voltage (V_0) at which $J_{\mathrm{ph}} = 0$ was determined [7].

In order to investigate the photocurrent in blends of BEH_1BMB_3-PPV:PCBM, knowledge about the hole and electron mobilities in the polymer and fullerene phases is indispensable. Recently, we have shown that electron and hole mobilities in a blend can be determined from dark current-voltage measurements by using suitable electrodes which suppress either holes or electrons [9]. In Fig. 1 the experimental electron and hole mobilities in 20:80 blends of BEH_1BMB_3-PPV:PCBM are shown as a function of temperature ($1/T$). It is observed that at room temperature the electron mobility in the PCBM phase ($\mu_e = 4 \times 10^{-3}$ cm^2/V s) is a factor of 125 larger than the hole mobility in the BEH_1BMB_3-PPV phase ($\mu_h = 3.2 \times 10^{-5}$ cm^2/V s). This low hole mobility originates from a hopping process between localized sites, which consist of conjugated polymer chain segments. Because of strong disorder there is a variation in the on-site energies, reducing the coupling between these localized states [10,11]. Since PPV and PCBM have different energetic disorders,

the activation energies of charge carrier mobility are different in the cases of electrons (0.18 eV) and of holes (0.35 eV). Consequently, as the temperature decreases, the difference between μ_e and μ_h becomes larger. For example, at 210 K the difference between experimental μ_e and μ_h increases to a factor of 2000, thereby strongly unbalancing the transport in these blends.

Figure 2 shows the experimental J_{ph} as a function of $V_0 - V$ in a 20:80 blend of BEH_1BMB_3-PPV:PCBM, for a temperature range of 210–295 K. It is observed that for $V_0 - V < 0.06$ V J_{ph} shows linear dependence on the voltage, due to the competition between drift and diffusion of photogenerated free charges to the electrodes [7]. However, above 0.06 V the experimental J_{ph} clearly shows a square-root dependence on the voltage for all measured temperatures, as is predicted by Eqs. (1) and (4) for very different μ_e and μ_h. Furthermore, as the temperature decreases, the square-root part of J_{ph} extends to larger voltages, since the difference between μ_e and μ_h becomes larger. At even larger voltages (≈ 0.8 V at 295 K) J_{ph} shows a clear transition to the saturation regime, where it becomes limited by the field and temperature dependence of the generation rate $G(E, T)$ [7]. These results are distinctly different from the case of OC_1C_{10}-PPV:PCBM blends, where no square-root dependence of J_{ph} is observed, as a result of more balanced transport [7]. The important question is whether J_{ph} from Fig. 2 is limited by the space charge [Eq. (4)] or by the mobility-lifetime product given by Eq. (1) The unique test to distinguish between the two processes is to investigate the dependence of J_{ph} on G, since a different dependence is predicted by Eqs. (1) and (4). A direct way to change the amount of photogenerated charge carriers is to vary the light intensity. We have recently demonstrated that in the absence of SCL the J_{ph} in reverse bias is described by $J_{ph} = qG(E, T)L$ [7]. Furthermore, for these non-SCL devices J_{ph} closely follows a linear dependence with light intensity [12,13]. Combining these two observations, it follows that G is proportional to light intensity in these types of devices. Therefore, the SCL photocurrent is expected to scale with a 3/4 power dependence on light intensity [Eq. (4)].

Figure 3 shows the $J_{ph} - (V_0 - V)$ characteristics, of the same device from Fig. 2, as a function of incident light power (ILP), measured at 210 K. This temperature was chosen because J_{ph} shows the largest square-root regime, but the same effect is present also at room temperature. The ILP was varied from 80 mW/cm^2 (upper curve) down to 6 mW/cm^2 using a set of neutral density filters. It appears from Fig. 3 that J_{ph} shows weaker light intensity dependence in the square-root regime as compared with the saturation regime. Figure 4(a) shows, in the double logarithmic plot, the experimental J_{ph} taken from Fig. 3 as a function of ILP for two different voltages, at $V_0 - V = 0.1$ V in the square-root regime and at $V_0 - V = 10$ V in the saturation regime. The slope S determined from the linear fit (lines) to the experimental data amount to $S = 0.76$ in the square-root part and $S = 0.95$ in the saturation part at high voltages. Furthermore, the SCL photocurrent predicted by Eq. (4) is compared with the square-root part of the experimental current in Fig. 3 (solid lines). Note that Eq. (4) contains parameters such as the charge carrier mobility of the slowest species (μ_h in this case), the relative dielectric permittivity ε_r of BEH_1BMB_3-PPV, and the generation rate G of e-h pairs. Since μ_h was experimentally measured (Fig. 1) and ε_r of 2.6 was found

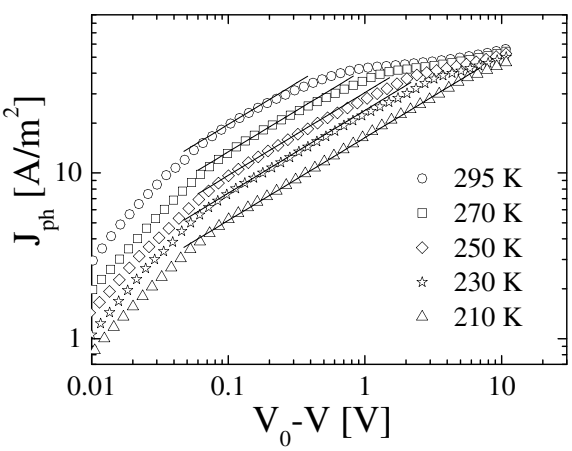

FIG. 2. Temperature dependence of the photocurrent (symbols) in a 20:80 blend of BEH_1BMB_3-PPV:PCBM versus effective applied voltage ($V_0 - V$) for a device of 275 nm thickness illuminated at an intensity of 80 mW/cm^2. The solid lines represent the square-root dependence of the photocurrent J_{ph} on effective voltage, used here as a guide for the eye.

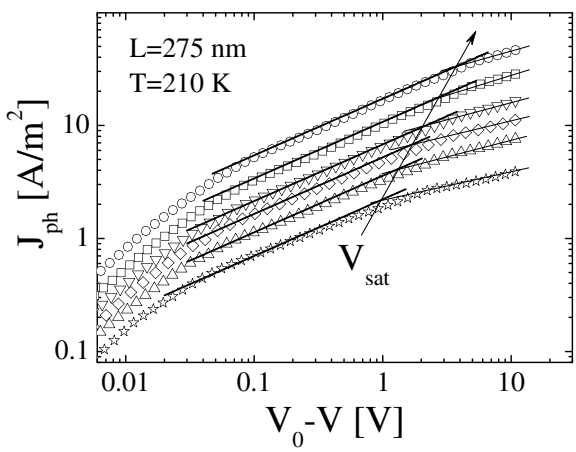

FIG. 3. Incident light power (ILP) dependence of the photocurrent (J_{ph}) versus the effective voltage ($V_0 - V$) measured at $T = 210$ K. The solid (thick) lines represent the calculated J_{ph} from Eq. (4) using $\mu_h = 1.2 \times 10^{-7}$ cm^2/V s, $\varepsilon_r = 2.6$, and $G \propto$ ILP, where ILP was varied from 80 to 6 mW/cm^2. The arrow indicates the voltage (V_{sat}) at which J_{ph} shows the transition to the saturation regime.

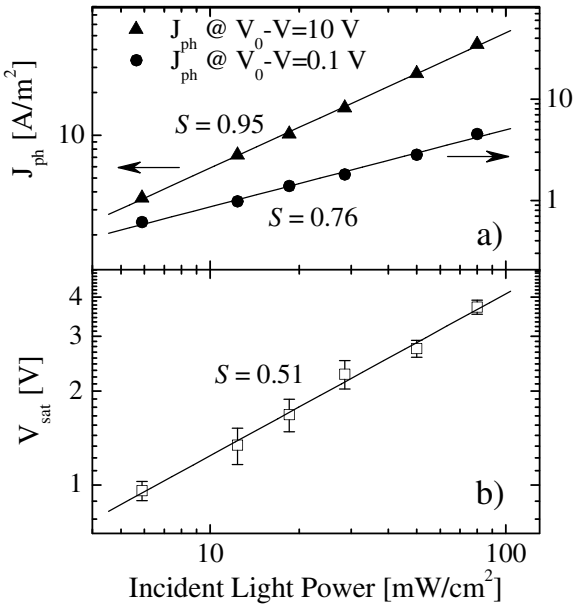

FIG. 4. (a) Incident light power (ILP) dependence of the photocurrent J_{ph} taken from Fig. 3 at an effective voltage of $V_0 - V = 0.1$ V and $V_0 - V = 10$ V (symbols). (b) Saturation voltage (V_{sat}) versus ILP as determined for Fig. 3. The slope (S) determined from the linear fit (solid lines) to the experimental data is written on the figure.

from impedance spectroscopy experiments, we can fit G at the highest light intensity. Using Eq. (4) we can predict the photocurrent at all other light intensities. As shown in Fig. 3, the predicted photocurrents (solid lines) are in excellent agreement with the experimental data. The $1/2$ power dependence of J_{ph} on voltage and the $3/4$ dependence on ILP are strong indications of the occurrence of a SCL photocurrent in this materials system.

Another way to confirm the presence of a SCL photocurrent is to consider the voltage V_{sat} at which J_{ph} switches from the square-root dependence to the saturation regime. This transition occurs when the hole accumulation region (L_1) becomes equal to the device thickness. From Eq. (3) it appears that in the case of a SCL photocurrent V_{sat} scales with the square root of light intensity. In contrast, in the absence of a space-charge limit [Eq. (1)] the transition voltage will be independent of the light intensity [1]. In Fig. 3 the voltage V_{sat} at which the transition occurs is determined from the crossover point of the square-root dependence and the extrapolated saturation part, as indicated by the arrow. From Fig. 3 it is already demonstrated that V_{sat} shows a clear variation with light intensity. In Fig. 4(b) V_{sat} is plotted in a double logarithmic scale as a function of ILP. A slope $S = 0.51$ is found, being in agreement with the space-charge limited prediction (of 0.5) from Eq. (3). This is a further conformation that the photocurrent in 20:80 blends of BEH_1BMB_3-PPV:PCBM devices is truly limited by space-charge effects. This SCL photocurrent is the maximum electrostatically allowed current that can be generated into the external circuit of any solar cell. A J_{ph} limited by space charge also has a strong impact on the power-conversion efficiency of this type of solar cells. For a photovoltaic device the fill factor is calculated from the ratio $100 \times J_{mp}V_{mp}/J_{sc}V_{oc}$, where J_{mp} and V_{mp} is the photocurrent and voltage at the maximum power point (where the J-V product is largest), J_{sc} the short-circuit current (applied voltage equals 0 V), and V_{oc} the open-circuit voltage. For a photocurrent varying with a $1/2$ power dependence on the applied voltage, the fill factor amounts to 42%. Since the photocurrent of a SCL device closely follows such a $V^{1/2}$ dependence [Eq. (4)], the maximum possible fill factor is limited to only 42%.

In summary, we demonstrated the existence of a fundamental limit of the photocurrent in semiconductors. The photocurrent in 20:80 blends of BEH_1BMB_3-PPV:PCBM solar cell devices reach this electrostatic limit already under normal operational conditions (0.8 Sun). The experimental photocurrents obey all features characteristic for the space-charge limited regime: The photocurrent is proportional with a $1/2$ power dependence on the voltage and a $3/4$ power of light intensity. Furthermore, the saturation voltage varies as the one-half power of the light intensity. These results give further insight into the mechanism of photoconduction in semiconductors and are valuable for the design of new materials in organic photovoltaic devices.

The authors are indebted to L. J. A. Koster for many valuable discussions and to J. C. Hummelen for the supply of the PCBM.

[1] A. M. Goodman and A. Rose, J. Appl. Phys. **42**, 2823 (1971).
[2] C. J. Brabec *et al.*, Adv. Funct. Mater. **11**, 15 (2001).
[3] M. M. Wienk *et al.*, Angew. Chem., Int. Ed. Engl. **42**, 3371 (2003).
[4] C. J. Brabec *et al.*, Chem. Phys. Lett. **340**, 232 (2001).
[5] T. Offermans *et al.*, J. Chem. Phys. **119**, 10 924 (2003).
[6] I. Montanari *et al.*, Appl. Phys. Lett. **81**, 3001 (2002).
[7] V. D. Mihailetchi, L. J. A. Koster, J. C. Hummelen, and P. W. M. Blom, Phys. Rev. Lett. **93**, 216601 (2004).
[8] C. Melzer *et al.*, Adv. Funct. Mater. **14**, 865 (2004).
[9] V. D. Mihailetchi *et al.*, Adv. Funct. Mater. (to be published).
[10] H. C. F. Martens, P. W. M. Blom, and H. F. M. Schoo, Phys. Rev. B **61**, 7489 (2000).
[11] H. Bässler, Phys. Status Solidi B **175**, 15 (1993).
[12] J. K. J. van Duren *et al.*, Adv. Funct. Mater. **14**, 425 (2004).
[13] P. Schilinsky, C. Waldauf, and C. J. Brabec, Appl. Phys. Lett. **81**, 3885 (2002).